Geometrical Nonlinear Analysis of Thick Plates with Rotation Fields by using Element-Free Galerkin Method

Yoshitaka Suetake[1], Masashi Iura[2], and S. N. Atluri[3]

Summary

In this paper, we treat with a nonlinear analysis of thick plates with rotation field. A moderately large rotation field is discussed here together with a small rotation field. When we simplify the large rotation field, we can derive a quite plain theory for thick plates, which is similar to von Karman's one. Numerical calculations are performed by using an element-free Galerkin method. The present EFGM is based on Lagrange polynomials and does not involve weight functions. As a numerical example, we adopt a nonlinear problem of thick plates, especially a snap-through problem of shallow convex plates.

Introduction

Involving a rotation field plays a key role in nonlinear analyses of continua. The variational formulations with rotation fields as variables have been extensively studied by one of the authors and his coworkers, [1]-[3]. In plate and shell problems, it is also very important to introduce rotation fields. Many authors have discussed a drilling rotation [4]-[8] in nonlinear shell theories. The authors [9]-[10] also dealt with finite deformed thick shell theories by introducing arbitrary rotation fields.

At this stage, it is quite interesting to overview a rotation field of thick plates and nonlinear plate theories. Since the geometry of plates is simpler than shells, we can easily overview the nonlinear theories of plates. Therefore we can easily make it clear what a role the rotation fields play in the nonlinear theory. A lot of thick plate theories have been presented by many authors [11]-[15]. Most of them are linear theories and do not involve rotation fields.

In this paper, we introduce two different rotation fields: one is a moderately large rotation field and the other small rotation field. Displacement fields are assumed to be large in both cases. As a numerical example, we adopt a snap-through problem of shallow convex plates. Then we employ an element-free Galerkin method (EFGM), which is formulated by using Lagrange polynomial [16].

---

[1] Ashikaga Institute of Technology, Ashikaga, Tochigi, 326-8558, JAPAN

[2] Tokyo Denki University, Hikigun, Saitama, 350-0394, JAPAN

[3] Center for Aerospace Research & Education, University of California, Irvine, Irvine, CA 92612, USA

Preliminaries

Let $\underline{\boldsymbol{X}}_0$ and $\underline{\boldsymbol{x}}_0$ to be position vectors of a generic point on the mid-surfaces before and after deformation. The base vectors defined at $\underline{\boldsymbol{X}}_0$ are $\underline{\boldsymbol{A}}_i$ $(i = 1 \sim 3)$, in which $\underline{\boldsymbol{A}}_\alpha$ $(\alpha = 1 \text{ or } 2)$ are the in-plane base vectors and $\underline{\boldsymbol{A}}_3$ is the normal to the mid-surfaces. Since we deal with a plate geometry, we can assume that all the base vectors before deformation are orthogonal and unit. At the same time, the base vectors in the undeformed plate domain can be defined as $\underline{\boldsymbol{G}}_i = \underline{\boldsymbol{A}}_i$.

Since $\underline{\boldsymbol{x}}_0 = \underline{\boldsymbol{X}}_0 + \underline{\boldsymbol{u}}_0$, base vectors after deformation can be written as

$$\underline{\boldsymbol{a}}_\alpha = \underline{\boldsymbol{x}}_0,_\alpha = \underline{\boldsymbol{X}}_0,_\alpha + \underline{\boldsymbol{u}}_0,_\alpha = \underline{\boldsymbol{A}}_\alpha + \underline{\boldsymbol{u}}_0,_\alpha = (\delta_{\alpha\beta} + u_{0\beta},_\alpha)\underline{\boldsymbol{A}}_\beta + u_{03},_\alpha \underline{\boldsymbol{A}}_3, \tag{1}$$

where $\underline{\boldsymbol{u}}_0 = u_{0i}\underline{\boldsymbol{A}}_i$ is a displacement vector on the mid-surface. On the other hand, when we discuss a map of $\underline{\boldsymbol{A}}_3$, namely $\underline{\boldsymbol{a}}_3$, a rotation field can be introduced. If we neglect thickness change of plates, $\underline{\boldsymbol{a}}_3$ must be unit. Therefore the mapping of $\underline{\boldsymbol{A}}_3$ to $\underline{\boldsymbol{a}}_3$ can be expressed by a rotation tensor $\underset{\sim}{\boldsymbol{R}}$ as

$$\underline{\boldsymbol{a}}_3 = \underset{\sim}{\boldsymbol{R}}.\underline{\boldsymbol{A}}_3. \tag{2}$$

In general, the rotation tensor $\underset{\sim}{\boldsymbol{R}}$ is written as

$$\underset{\sim}{\boldsymbol{R}} = \underset{\sim}{\boldsymbol{I}} + \frac{\sin\theta}{\theta}\underline{\boldsymbol{\omega}} \times \underset{\sim}{\boldsymbol{I}} + \frac{1-\cos\theta}{\theta^2}\underline{\boldsymbol{\omega}} \times (\underline{\boldsymbol{\omega}} \times \underset{\sim}{\boldsymbol{I}}). \tag{3}$$

where $\underline{\boldsymbol{\omega}}$ is a rotation vector and $\theta = \sqrt{\underline{\boldsymbol{\omega}} \cdot \underline{\boldsymbol{\omega}}}$ is a rotation angle [9]-[10].

We introduce here the Mindlin assumption, that is, a straight fiber normal to the undeformed mid-surface is mapped into an another straight fiber after deformation. Therefore a generic point $\underline{\boldsymbol{X}} = \underline{\boldsymbol{X}}_0 + \xi_3\underline{\boldsymbol{A}}_3$ in the undeformed plate domain is mapped into a point $\underline{\boldsymbol{x}} = \underline{\boldsymbol{x}}_0 + \xi_3\underline{\boldsymbol{a}}_3$ after deformation. Consequently, base vectors at the generic point in the deformed plate domain is given by

$$\underline{\boldsymbol{g}}_\alpha = \underline{\boldsymbol{a}}_\alpha + \xi^3\underline{\boldsymbol{a}}_3,_\alpha \quad , \quad \underline{\boldsymbol{g}}_3 = \underline{\boldsymbol{a}}_3. \tag{4}$$

Rotation Fields

The rotation tensor $\underset{\sim}{\boldsymbol{R}}$ represents a rigid rotation. In the rigid rotation process, we can select arbitrary rotation paths. Namely, a rotation vector can be selected arbitrarily. However, if we adopt the rotation vector $\underline{\boldsymbol{\omega}}$ so that it becomes a normal to the circle made by the base vectors $\underline{\boldsymbol{A}}_3$ and $\underline{\boldsymbol{a}}_3$ as shown in Fig.1, the rigid rotation can be determined uniquely. Then, since $\underline{\boldsymbol{\omega}}$ is perpendicular to $\underline{\boldsymbol{a}}_3$, it can be expressed by only two components:

$$\underline{\boldsymbol{\omega}} = \omega_\alpha \underline{\boldsymbol{A}}_\alpha \quad ; \quad \theta^2 = (\omega_1)^2 + (\omega_2)^2 . \tag{5}$$

In this paper, we introduce two different rotation fields: one is a moderately large rotation field and the other small rotation field. In the moderately large rotation field, we neglect higher order terms of θ^2 . Therefore we can approximate Eq.(3) and obtain an approximate expression of $\underline{\boldsymbol{a}}_3$:

$$\underset{\sim}{\boldsymbol{R}} \approx \underset{\sim}{\boldsymbol{I}} + \underline{\boldsymbol{\omega}} \times \underset{\sim}{\boldsymbol{I}} + \frac{1}{2} \underline{\boldsymbol{\omega}} \times (\underline{\boldsymbol{\omega}} \times \underset{\sim}{\boldsymbol{I}}) , \tag{6}$$

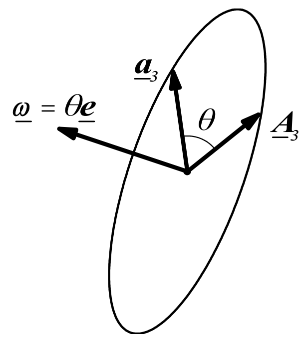

Fig.1 Rotation Vector

$$\underline{\boldsymbol{a}}_3 = \omega_2 \underline{\boldsymbol{A}}_1 - \omega_1 \underline{\boldsymbol{A}}_2 + (1 - \frac{\theta^2}{2}) \underline{\boldsymbol{A}}_3 . \tag{7}$$

Note that Eq.(7) satisfies the condition of $\underline{\boldsymbol{\omega}}.\underline{\boldsymbol{a}}_3 = 0$. In the small rotation field, we neglect higher order terms of θ in Eqs.(6) and (7).

From Eq.(7), we obtain the derivative of $\underline{\boldsymbol{a}}_3$ in the moderately large rotation field as

$$\underline{\boldsymbol{a}}_3,_\alpha = e_{\beta\gamma} \omega_\gamma,_\alpha \underline{\boldsymbol{A}}_\beta - \theta\theta,_\alpha \underline{\boldsymbol{A}}_3 = e_{\beta\gamma} \omega_\gamma,_\alpha \underline{\boldsymbol{A}}_\beta - \omega_\gamma \omega_\gamma,_\alpha \underline{\boldsymbol{A}}_3 \tag{8}$$

where $e_{\alpha\beta}$ is a permutation symbol. The expression for $\underline{\boldsymbol{a}}_3,_\alpha$ in the small rotation field is obtained by neglecting the second term in Eq.(8).

Strain Components and Variational Principle

We employ the Green's strain tensor as a strain measure here. If we assume that u_{03} □ ω_α □ $u_{0\alpha}$, we obtain the Green's strain components on the mid-surface, ε_{0ij} , and in the plate domain, ε_{ij} , as follows:

$$\varepsilon_{0\alpha\beta} \approx \frac{1}{2}(u_{0\beta},_\alpha + u_{0\alpha},_\beta + u_{03},_\alpha u_{03},_\beta) \ , \ \varepsilon_{0\alpha 3} = \varepsilon_{03\alpha} \approx \frac{1}{2}(e_{\alpha\beta}\omega_\beta + u_{03},_\alpha) \ , \ \varepsilon_{033} \approx 0 , \tag{9}$$

$$\varepsilon_{\alpha\beta} \approx \varepsilon_{0\alpha\beta} + \frac{\xi_3}{2}(\varepsilon_{\alpha\gamma}\omega_\gamma,_\beta + \varepsilon_{\beta\gamma}\omega_\gamma,_\alpha) \ , \ \varepsilon_{\alpha 3} = \varepsilon_{3\alpha} = \varepsilon_{03\alpha} - \underline{\underline{\xi_3 \omega_\beta \omega_\beta,_\alpha}} \ , \ \varepsilon_{033} \approx 0 . \tag{10}$$

where the underlined term is negligible in the small rotation field. When we consider initial deflection w_0 , the first of Eq.(9) is modified as

$$\varepsilon_{0\alpha\beta} \approx \frac{1}{2}(u_{0\beta},_{\alpha} + u_{0\alpha},_{\beta} + u_{03},_{\alpha} u_{03},_{\beta} + w_0,_{\alpha} u_{03},_{\beta} + u_{03},_{\alpha} w_0,_{\beta}) . \tag{11}$$

By using these strain components, we obtain a total potential energy of thick plate problems as

$$\begin{aligned} \Pi = \frac{1}{2}\int_{-b}^{b}\int_{-a}^{a}[\frac{Et}{1-\nu^2}\{\varepsilon_{01}{}^2 + \varepsilon_{02}{}^2 + 2\nu\varepsilon_{01}\varepsilon_{02} + 2(1-\nu)\varepsilon_{12}{}^2\} \\ +D\{\rho_1{}^2 + \rho_2{}^2 + 2\nu\rho_1\rho_2 + 2(1-\nu)\rho_{12}{}^2\} + \kappa Gt\{(u_{03},_1 + \omega_2)^2 + (u_{03},_2 - \omega_1)^2\}]d\xi d\eta \, . \\ -\int_{-1}^{1}\int_{-1}^{1}(\bar{X}_i u_{0i})d\xi d\eta \end{aligned} \tag{12}$$

where $\bar{X}_i$ are components of a load vector and ρ_1, ρ_2, and ρ_{12} mean curvatures of a plate defined as

$$\rho_1 \equiv -\omega_2,_1 \quad , \quad \rho_2 \equiv \omega_1,_2 \quad , \quad \rho_{12} \equiv \omega_1,_1 - \omega_2,_2 \, . \tag{13}$$

In numerical analyses, we discretize the functional (12) and derive a governing equation through the variational principle.

Element-Free Galerkin Method

In the discretization process we use an element-free Galerkin method based on Lagrange polynomial [16]. In the beginning we introduce a square support region Ω with a side length 2ρ around an evaluation point (x,y) as shown in Fig.2. If $(N+1)^2$ nodal points (x_i, y_i) $(i = 0 \sim N)$ are distributed as lattice points in Ω, we can express the solution at (x,y) by using the following Lagrange polynomial:

$$f(x,y) = \sum_{i=0}^{N}\sum_{j=0}^{N} f_{ij}\varphi_i(x)\psi_j(y) \, . \tag{14}$$

where $\varphi_i(x)$ and $\psi_j(y)$ are one-dimensional Lagrange bases, which satisfy the matching condition: $\varphi_i(x_k) = \delta_{ik}$ and $\psi_j(y_l) = \delta_{jl}$. When using Eq.(14), we can represent the solution and its derivatives at the evaluation point by the following discretized form:

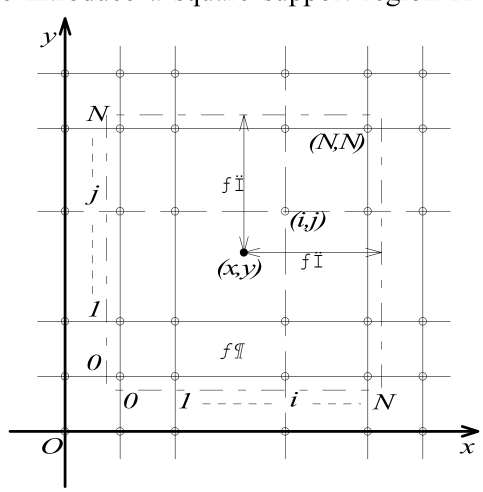

Fig.2 Two-Dimensional Support

$$\partial_x^m \partial_y^n f(x,y) = \underline{\boldsymbol{B}}_r(x,y)^T . \underline{\boldsymbol{f}} \, . \tag{15}$$

where $\underline{f}$ is a nodal value vector within the support Ω and $\underline{\boldsymbol{B}}_r$ are differential operation vectors, which consist of the Lagrange bases and their derivatives. We should note that the finite element subdivision is not required in the above discretization process.

Numerical Example

As a numerical example we adopt a snap-through problem of a shallow convex plate as shown in Fig.3. Numerical properties of the model are as follows: Poisson's ratio ν is 0.3 ; the width-thickness ratio $\zeta \equiv t/a$ is 0.6 ; the initial deflection at center point w_{C0}/t is 1.0. The EFGM parameters are as follows: total nodes are $11 \times 11 = 121$; number of cells is $5 \times 5 = 25$; the support parameter ρ is 0.6 ; the order of Gaussian quadrature is 8. In the nonlinear calculation we adopt the displacement control scheme.

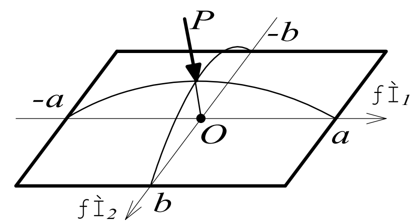

Fig.3 Shallow Convex Plate

Numerical results are shown in Fig.4, which shows the relationship between a non-dimensional load parameter $\Gamma \equiv Pa/D$ and a non-dimensional deflection $d_C \equiv u_{03}/t$ at the center point of the plate. In Fig.4, the solid line indicates a result of a thin plate analysis and the plots that of a thick plate analysis. Apparently different results are obtained from both approaches.

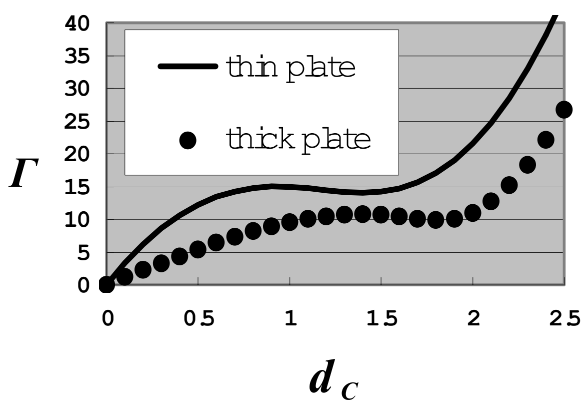

Fig.4 Load-Deflection Curve of Snap-Through

References

1 Atluri, S. N. and Murakawa, H. (1977), "On hybrid finite element models in nonlinear solid mechanics", *Finite Elements in Nonlinear Mechanic* (edited by Bergan, P. G. et al.), Vol.1, pp.3-41.

2 Iura, M. and Atluri, S. N. (1992), "Formulation of a membrane finite element with drilling degrees of freedom", *Computational Mechanics*, Vol.9, pp.417-428.

3 Atluri, S. N. and Cazzani, A. (1995), "Rotations in computational solid mechanics", *Archives of Computational Methods in Engineering*, Vol.2, No.1, pp.49-138.

4 Atluri, S. N. (1984), "Alternate stress and conjugate strain measures, and mixed variational formulations involving rigid rotations, for computational analyses of finitely deformed solids, with application to plates and shells – I", *Computer & Structures*, Vol.18, pp.93-116.

5 Simo, J. C. and Fox, D. D. (1989), "On a stress resultant geometrically exact shell model. Part I: Formulation and optimal parametrization", *Computer Methods in Applied Mechanics and Engineering*, Vol.72, pp.267-304.

6 Sansour, C. and Bufler, H. (1992), "An exact finite rotation shell theory, its mixed variational formulation and its finite element implementation", *International Journal for Numerical Methods in Engineering*, Vol.34, pp.73-115.

7 Chroscielewski, J., Makowski, J., and Stumpf, H. (1992), "Genuinely resultant shell finite elements accounting for geometric and material nonlinearity", *International Journal for Numerical Methods in Engineering*, Vol.35, pp.63-94.

8 Ibrahimbegovic, A. (1994), "Stress resultant geometrically nonlinear shell theory with drilling rotations – Part I. A consistent formulation", *Computer Methods in Applied Mechanics and Engineering*, Vol.118, pp.265-284.

9 Suetake, Y., Iura, M., and Atluri, S. N. (1999), "Shell Theories with Drilling Degrees of Freedom and Geometrical and Material Assumptions", *Computer Modeling and Simulation in Engineering*, Vol.4, No.1, pp.42-49.

10 Suetake, Y., Iura, M., and Atluri, S. N. (2003), "Variational Formulation and Symmetric Tangent Operator for Shells with Finite Rotation Field", *Computer Modeling in Engineering & Science*, Vol.4, No.2, pp.329-336.

11 Reissner, E. (1945), "The Effect of Transverse Shear Deformation on the Bending of Elastic Plates", *Journal of Applied Mechanics*, Vol.12, pp.A69-A77.

12 Mindlin, R. D. (1951), "Influence of Rotatory Inertia and Shear on Flexural Motions of Isotropic, Elasitc Plates", *Journal of Applied Mechanics*, Vol.18, pp. 31-38.

13 Lo, K. H., Christensen, R. M., and Wu, E. M. (1977), "A High Order Theory of Plate Deformation – I. Homogeneous Plates", *Journal of Applied Mechanics*, Vol.44, pp.663-668.

14 Hirashima, K. and Negishi, Y., "Some Considerations on Accuracies of Typical Two-Dimensional Plate Theories including the Effects of Transverse Components", *Proceedings of JSCE*, Vol.330, pp.1-14, 1983.

15 Koga, T., "High-Order Theory for Plate Bending", *Transactions of JSME (Series A)*, Vol.48, No.433, pp.1151-1159, 1982.

16 Suetake, Y. (2002), "Element-Free Galerkin Method Based on Lagrange Polynomial", *Journal of Engineering Mechanics*, Vol.128, No.2, pp.231-239.